

Communication

# Multi-Frequency Doppler Velocimetry Based on a Mode-Locked Distributed Bragg Reflector Laser

Hao Song<sup>1,2,3</sup>, Dan Lu<sup>1,2,3,\*</sup>, Zhihao Zhang<sup>1,2,3</sup>, Fei Guo<sup>1,2,3</sup>, Daibing Zhou<sup>1,2,3</sup> and Lingjuan Zhao<sup>1,2,3</sup>

<sup>1</sup> Key Laboratory of Semiconductor Materials Science, Institute of Semiconductors, Chinese Academy of Sciences, Beijing 100083, China; songhao@semi.ac.cn (H.S.); zhangzhihao20@semi.ac.cn (Z.Z.); guofei11@semi.ac.cn (F.G.); dbzhou@semi.ac.cn (D.Z.); ljzhao@semi.ac.cn (L.Z.)

<sup>2</sup> Center of Materials Science and Optoelectronics Engineering, University of Chinese Academy of Sciences, Beijing 100049, China

<sup>3</sup> Beijing Key Laboratory of Low Dimensional Semiconductor Materials and Devices, Beijing 100083, China

\* Correspondence: ludan@semi.ac.cn

**Abstract:** A differential multi-frequency laser Doppler velocimetry is demonstrated, utilizing the synchronized multimode of a mode-locked distributed Bragg reflector laser. This scheme enables the simultaneous detection of multiple Doppler frequency shifts. Multiple differential Doppler shifts of 0.6 Hz, 1.3 Hz, and 1.9 Hz are obtained, with an average speed of 3.677 mm/s and a standard deviation of 0.122 mm/s, demonstrating a cross-referenced velocity measurement capability. The measurement results are also compared with the dual-frequency laser Doppler velocimetry scheme using electro-optical modulation.

**Keywords:** differential doppler velocimetry; distributed Bragg reflector; mode-locked laser



Citation: Song, H.; Lu, D.; Zhang, Z.; Guo, F.; Zhou, D.; Zhao, L. Multi-Frequency Doppler Velocimetry Based on a Mode-Locked Distributed Bragg Reflector Laser. *Photonics* **2023**, *10*, 1254. <https://doi.org/10.3390/photonics10111254>

Received: 9 October 2023

Revised: 7 November 2023

Accepted: 10 November 2023

Published: 13 November 2023



**Copyright:** © 2023 by the authors. Licensee MDPI, Basel, Switzerland. This article is an open access article distributed under the terms and conditions of the Creative Commons Attribution (CC BY) license (<https://creativecommons.org/licenses/by/4.0/>).

## 1. Introduction

Doppler lidar has been widely used in the military, meteorology [1], aviation [2], and environmental monitoring, due to its advantages in non-contact measurement, high precision, and robust resistance to interference. Conventional Doppler lidar uses a single-frequency laser to detect the Doppler frequency shift of a moving object. Such a single-frequency laser Doppler velocimetry (SF-LDV) imposes stringent requirements on the laser linewidth, and is susceptible to noise caused by the scattering from rough target surfaces and atmospheric turbulence [3], limiting the accuracy of the measurement [4]. To address this issue, a solution known as dual-frequency laser Doppler velocimetry (DF-LDV) has been proposed, which involves measuring the Doppler frequency difference between two modes. This approach employs two phase-correlated laser modes as the probing signal, effectively translating the strict requirement for laser linewidth to the frequency difference between two synchronized laser modes [5–7]. The measurement accuracy depends on the microwave linewidth instead of the optical linewidth [8]. The precision of the differential Doppler shift (DDS) measurement can reach a sub-Hertz level when the laser modes are synchronized using an external Radio Frequency (RF) source [9,10]. The two laser modes can be obtained through various methods, such as electro-optical modulation sidebands [11,12], injection-locked semiconductor laser's period oscillation modes [13], or the dual modes of a monolithically integrated dual-mode amplified feedback laser [10]. Alternatively, dual-frequency laser can also be obtained by filtering two modes from a multimode laser, such as mode locked laser (MLL) [14].

In addition to DF-LDV, differential Doppler velocimetry can also be realized using more laser modes, which can be referred to as multi-frequency laser Doppler velocimetry (MF-LDV). This technique makes use of multiple synchronized laser modes to obtain multiple DDS components simultaneously, as compared to DF-LDV, which only has a single DDS component. The multiple DDS components can be cross-referenced to enhance

the measurement robustness and offer more flexibility in signal processing and error correction. Additionally, it is possible to calculate the confidence of the speed measurement from the multiple DDS components. If the multiple laser modes are oriented in different directions, the MF-LDV can also provide information about the velocity components in various directions. When the multiple laser modes are locked in phase, such as in a mode-locked state, the probing signal also manifests as a short pulse train in the time domain. Similar to pulsed radar, the detection range of an MF-LDV in a mode-locked state can be extended when using a short pulse, due to its high peak power capability. Amplification is more effective when short pulses are used. While there have been reports exploring velocity measurement with mode-locked lasers, these studies have primarily focused on single-wavelength or dual-wavelength measurements [14,15]. There are very few, if any, reports on using multiple modes of an MLL for differential Doppler velocity measurements.

In this paper, we propose and demonstrate an MF-LDV scheme using a monolithically integrated mode-locked distributed Bragg reflector laser diode (DBR-MLLD). The DBR structure limits the number of synchronized modes to ensure that each mode contains sufficient power for probing. Furthermore, in contrast to traditional MLL, the overall optical spectrum bandwidth of the DBR-MLLD can be limited to a narrow span, facilitating an efficient amplification when using a boosting amplifier. A DBR-MLLD was first fabricated to generate short pulse at a picosecond level. Subsequently, it was used in an MF-LDV experiment for detecting multiple DDSs. Three sets of DDSs were obtained at frequencies of 0.6 Hz, 1.3 Hz, and 1.9 Hz. These frequencies corresponded to an average speed of 3.677 mm/s, with a standard deviation of 0.122 mm/s. At the same time, the mode-locked laser itself is in pulsed form, and the possibility of using pulsed ranging exists [16]. The measurement was also compared with DF-LDV scheme using an electro-optical modulation method.

### 2. Principle

Figure 1a illustrates the schematic configuration of the MF-LDV system. The multi-frequency light is split into two channels via an output coupler, one is the probe light and the other is reference light. The probe light is sent out and collected using an optical circulator and a collimator. The back-reflected signal light combines with the reference light at the receiver for coherent detection. Digital processing follows the detection to obtain the DDS components.

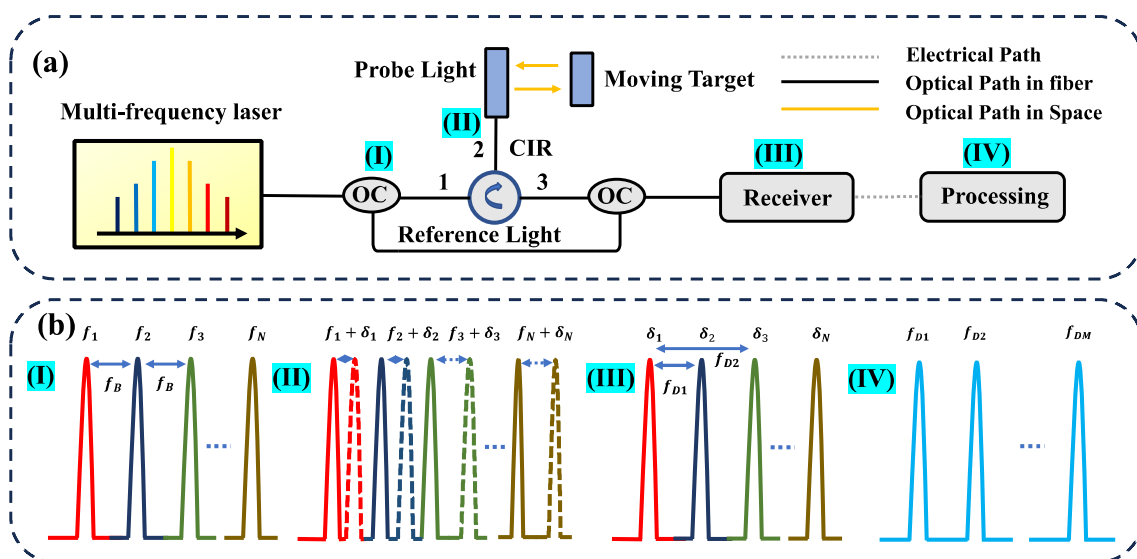


**Figure 1.** Schematic setup of the MF-LDV and its working principle. (a) Schematic setup of the MF-LDV. (b) The brief principle of the MF-LDV. OC: output coupler; CIR: circulator.

The principle of the multi-frequency Doppler velocity measurement is shown in Figure 1b (labeled as (I)–(IV)). When the multiple probing laser modes with a carrier frequencies of  $f_1, f_2 \dots f_N$  are reflected from a moving object, they will experience the Doppler shifts of  $f_1 + \delta_1, f_2 + \delta_2 \dots f_N + \delta_N$  for each mode [6], where  $\delta_1 = 2sf_1/c, \delta_2 = 2sf_2/c \dots \delta_N = 2sf_N/c$ . The velocity of the object can be obtained as:

$$s = f_{DM}c/2f_{BM} \tag{1}$$

$$f_{DM} = \delta_N - \delta_{N-M} (M < N) \tag{2}$$

where  $f_{DM}$  is the DDS when using the  $N^{\text{th}}$  and the  $(N-M)^{\text{th}}$  laser modes as the probe light,  $f_{BM}$  is the beat frequency of the two modes,  $c$  is the speed of light in vacuum. It can be found that the speed can be determined by measuring the DDS of the laser modes with a mode spacing of  $f_{BM}$ . Assuming that there are four modes of participation in speed measurement, we can obtain the differential Doppler shifts between different mode intervals. For instance,  $\delta_2 - \delta_1, \delta_3 - \delta_2$ , and  $\delta_4 - \delta_3$  correspond to the fundamental frequency differential Doppler shift  $f_{D1}$ . In addition,  $\delta_3 - \delta_1, \delta_4 - \delta_2$  correspond to the frequency-doubled differential Doppler shift  $f_{D2}$ . Moreover,  $\delta_4 - \delta_1$  corresponds to a frequency-tripled differential Doppler shift  $f_{D3}$ . The measurable DDS is influenced by the phase correlation between laser modes, rather than by the laser linewidth, as is the case with SF-LDV measurement. For MF-LDV using a MLLD, hybrid mode locking can greatly improve the phase correlation among laser modes, leading to a reduction in the beating RF linewidth to the Hertz level. The measurement precision can be comparable to that of the SF-LDV using lasers with extremely narrow linewidth. The minimum detectable speed and measurement efficiency are influenced by the mode spacing. A larger mode spacing will result in a higher DDS for the same moving speed. This means that in the case of low-speed detection, a larger mode spacing will result in a shorter oscillation period in the detected waveform envelope when calculating DDS, relaxing the pressure on data acquisition depth. For the same DDS, a larger mode spacing will result in a higher speed resolution. Table 1 shows the DDS for a speed of 1.5 m/s and the speed resolution for a DDS of 1 Hz when the mode spacings are changed from 100 MHz to 100 GHz. For adjacent mode spacing in the MHz to GHz range, fiber or solid-state mode-locked lasers can be used. However, for adjacent mode spacing beyond 10 GHz, a semiconductor based MLLD would be a more suitable and practical solution.

**Table 1.** Detectable DDS at a speed of 1.5 m/s and the speed resolution for a DDS of 1 Hz at different mode spacings.

Mode Spacing (Hz)	DDS (Hz) for Speed of 1.5 m/s	Speed Resolution (m/s) for DDS of 1 Hz
100 M	1	1.5
1 G	10	0.15
10 G	100	0.015
20 G	200	0.0075
100 G	1000	0.0015

### 3. Device Characterization and Experimental Results

A DBR-MLLD was fabricated to demonstrate the MF-LDV scheme. The DBR-MLLD used in the experiment had a cavity length of 1700  $\mu\text{m}$ , corresponding to a mode spacing about 25 GHz. The lengths of the DBR section, gain section, and saturated absorber (SA) section were 150  $\mu\text{m}$ , 1450  $\mu\text{m}$ , and 70  $\mu\text{m}$ , respectively. Laser was coupled out from the DBR section. An RF signal was applied to the SA section for hybrid mode locking. The DBR section and the facet of the SA section form a wavelength-selective cavity, generating only a few modes supported by the DBR mirror. The DBR-MLLD was packaged in a butterfly module for device characteristics and speed measurement as shown in Figure 2.

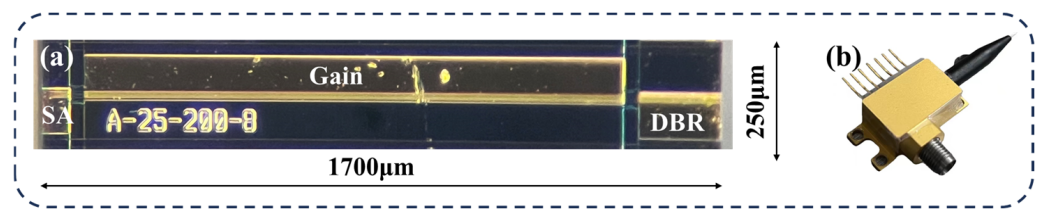


**Figure 2.** Photographs of DBR-MLLD. (a) Photograph of laser. (b) Photograph after butterfly package.

The device characterization set-up for the DBR-MLLD is shown in Figure 3. The laser output passed through a 90:10 optical coupler, where 10% of the light was used for optical spectrum analysis using an Optical Spectrum Analyzer (OSA), and 90% of the light was sent to an Electronic Spectrum Analyzer (ESA) for RF spectral analysis and a Second Harmonic Generation (SHG) autocorrelator for pulse characterization after amplification using an Erbium-Doped Fiber Amplifier (EDFA).

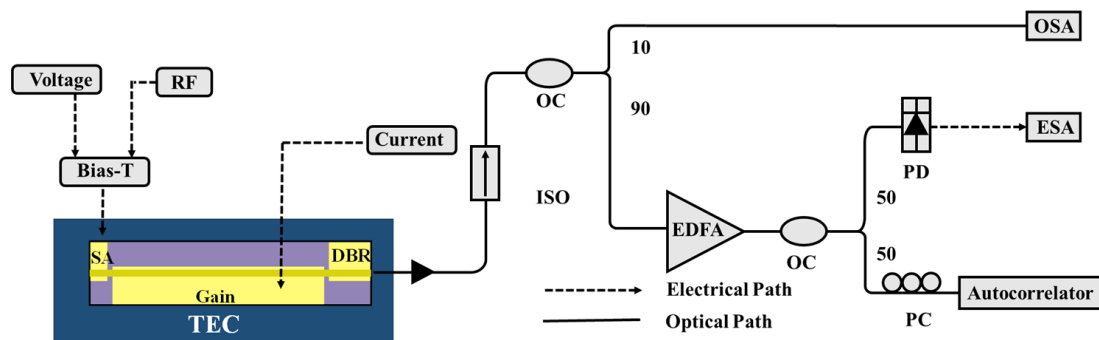


**Figure 3.** Pulse measurement set-up of the DBR-MLLD. RF: Radio Frequency; SA: saturated absorber; DBR: distributed Bragg reflector; TEC: thermoelectric cooler; EDFA: erbium-doped fiber amplifier; ISO: isolator; PD: photodetector; OC: optical coupler; OSA: optical spectrum analyzer; ESA: electronic spectrum analyzer; PC: polarization controller.

During the measurement, the gain section was biased at 350 mA and the SA section was reverse biased at  $-2$  V. This configuration allowed for the generation of short optical pulses with a repetition rate of approximately 25 GHz. Figure 4a shows the optical spectrum of the DBR-MLLD, revealing the presence of only four modes within the  $-3$  dB range. Furthermore, the spectral width within the  $-20$  dB range is about 2.5 nm. The presence of a limited number of oscillation modes and the narrow spectral range will contribute to an enhanced efficiency in optical amplification. For comparison, Figure 4b displays the optical spectrum of a Fabry-Pérot MLLD, where in the  $-20$  dB spectral width covers approximately 23 nm. Figure 5a shows the RF spectrum of the DBR-MLLD after hybrid mode locking, revealing a repetition frequency of 25.613 GHz. The beating signal is 35-dB stronger than the noise pedestal, indicating a good phase correlation among the oscillation modes. Figure 5b,c depict the optical pulse autocorrelation traces over a span of 50 ps and 150 ps, respectively. The full width at half maximum (FWHM) of the optical pulse autocorrelation trace with a 50 ps span is measured to be 9.07 ps, which corresponds to a pulse width of 4.535 ps, assuming a Lorentzian line shape.

Then the DBR-MLLD was applied to the differential Doppler velocity measurement, as shown in Figure 6. The moving object was a small mirror mounted on an electrically controlled motor, with a speed ranging from 1 mm/s to 100 mm/s. The DBR-MLLD was biased under the same condition as during the device characterization. Coherent detection was achieved by using a balanced detector, and the waveform was captured using a real-time oscilloscope (OSC). Figure 7a shows the waveform of detected waveform after coherent detection. The waveform takes a pulsed form, due to the pulsed nature of the probe light.

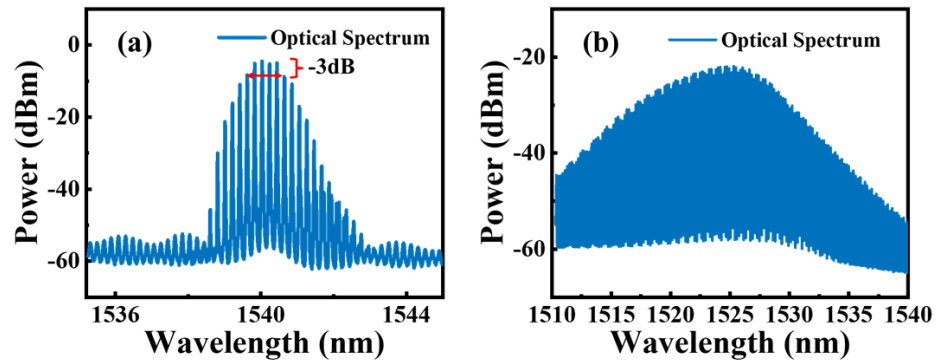


Figure 4. (a) Optical spectrum of the DBR-MLLD. (b) Optical spectrum of the Fabry-Pérot MLLD.

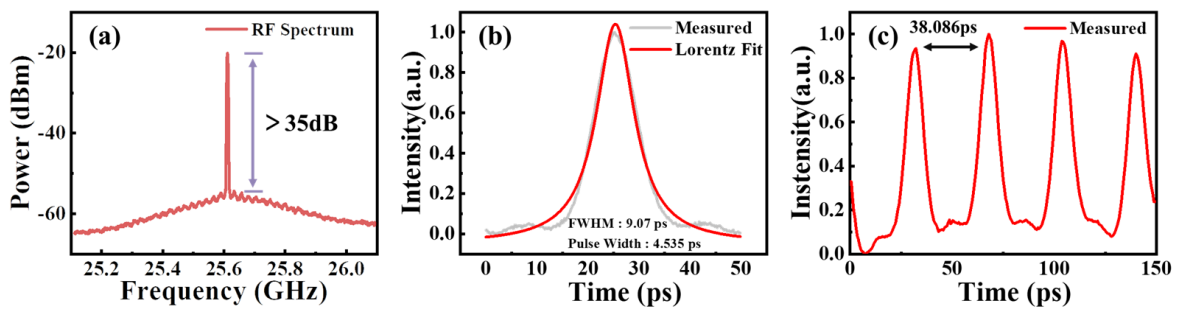


Figure 5. The optical spectrum and autocorrelation traces of the DBR-MLLD. (a) Optical spectrum. (b) Autocorrelation traces in a 50 ps span and (c) autocorrelation traces in a 150 ps span.

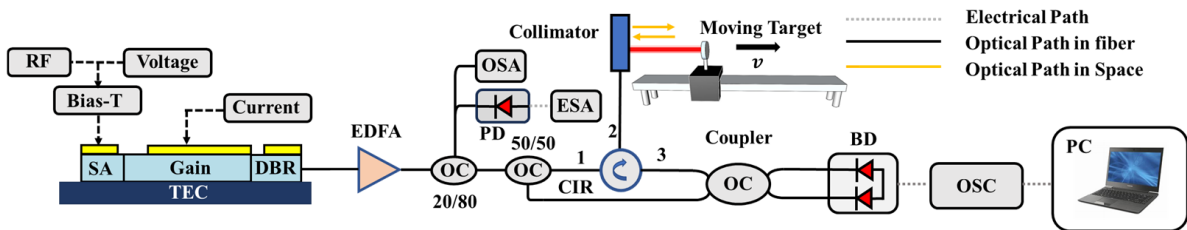


Figure 6. Schematic of the MF-LDV based on DBR-MLLD. BD: balanced photodetector; OSC: oscilloscope; PC: personal computer.

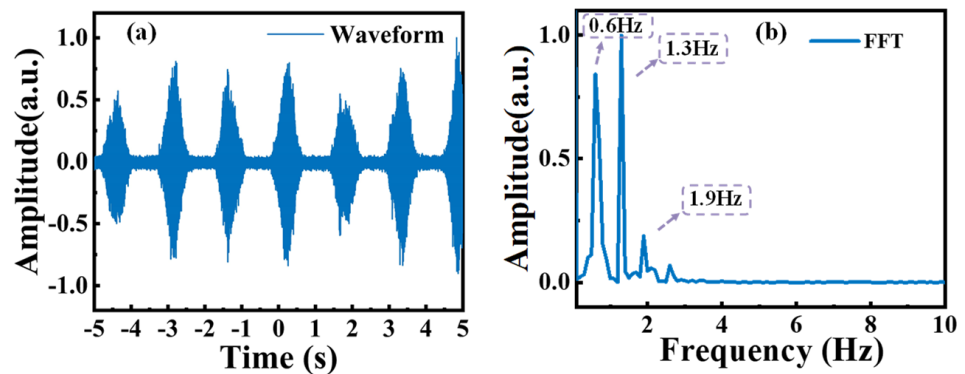


Figure 7. (a) Normalized temporal waveform of the MF-LDV. (b) Normalized power spectrum of the Doppler signal.

It is different from the waveform of a dual-frequency scheme, which typically manifests as a sinusoidal waveform. In order to obtain the DDS information, the time-domain waveforms were squared and then subjected to the Fast Fourier Transform (FFT). The data

acquisition time window was set to 10 s, allowing for a frequency resolution of approximately 0.1 Hz. Figure 7b shows the DDS components calculated from the waveform. Three DDS components can be observed at 0.6 Hz, 1.3 Hz, and 1.9 Hz, corresponding to the fundamental, frequency-doubled, and frequency-tripled differential Doppler frequency, respectively. It can also be deduced that there were four modes that took effect during the measurement. The moving speed calculated from the three DDSs are 3.514 mm/s, 3.807 mm/s, and 3.709 mm/s, respectively, using Equation (1). The calculated average speed is 3.677 mm/s, with a standard deviation of 0.122 mm/s.

Subsequently, a DF-LDV experiment was conducted to compare the MF-LDV and DF-LDV schemes. The dual modes in the DF-LDV experiment were obtained by modulating a continuous-wave laser using a Mach-Zehnder modulator. The modulator was biased in a carrier suppression state, driven by a 12.5 GHz RF signal. Figure 8a shows the optical spectrum of the generated two modes with a carrier suppression ratio of over 20 dB. Figure 8b,c depict the 25 GHz beat frequency signal and the corresponding time-domain waveform, respectively. A sinusoidal wave can be observed. Then the time domain waveform was squared and subjected to a Fast Fourier Transform. A single DDS component of 0.6 Hz was obtained, as shown in Figure 8d. This corresponds to a speed of 3.6 mm/s, matching what was obtained using the DBR-MLLD.

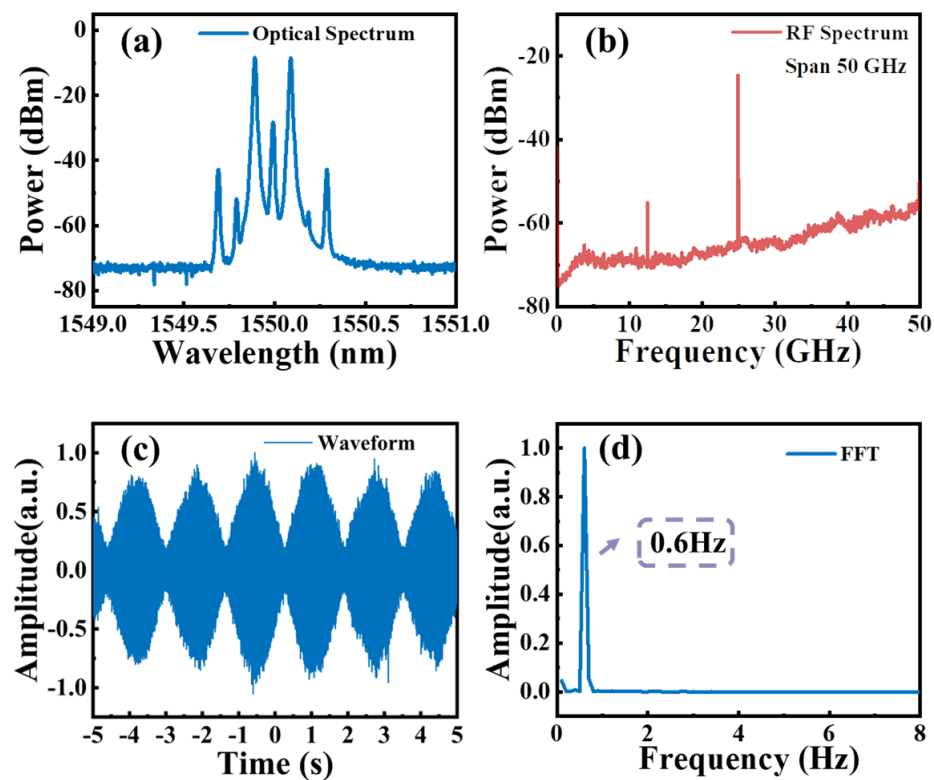


Figure 8. (a). Normalized temporal waveform of the DF-LDV. (b) Optical spectrum in carrier suppressed state. (c) RF spectrum. (d) Normalized power spectrum of the Doppler signal.

#### 4. Conclusions

In summary, we have proposed and demonstrated a multi-frequency laser Doppler velocimetry using a DBR-MLLD. Compared to a DF-LDV scheme, the MF-LDV scheme enables a cross-referenced measurement capability, ensuring robust speed detection. The pulsed operation property and limited number of oscillation modes of the DBR-MLLD provides a long-range detection capability. Multiple DDSs of 0.6 Hz, 1.3 Hz, and 1.9 Hz, were obtained, with an average speed of 3.677 mm/s, and standard deviation of 0.122 mm/s.

**Author Contributions:** Conceptualization, D.L. and H.S.; methodology, H.S.; formal analysis, H.S. and Z.Z.; investigation, H.S.; resources, D.L. and L.Z.; data curation, H.S.; writing—original draft preparation, H.S.; writing—review and editing, D.L., F.G. and H.S.; visualization, H.S.; supervision, D.L. and L.Z.; funding acquisition, D.L. and D.Z. All authors have read and agreed to the published version of the manuscript.

**Funding:** The work is supported by National Natural Science Foundation of China (61975197); the Strategic Priority Research Program of Chinese Academy of Sciences XDB43000000.

**Institutional Review Board Statement:** Not applicable.

**Informed Consent Statement:** Not applicable.

**Data Availability Statement:** Data are contained within the article.

**Conflicts of Interest:** The authors declare no conflict of interest.

## References

1. Vaughan, J.M. Coherent Laser Spectroscopy and Doppler Lidar Sensing in the Atmosphere. *Phys. Scr.* **1998**, *T78*, 73. [[CrossRef](#)]
2. Thobois, L.; Cariou, J.P.; Gultepe, I. Review of Lidar-Based Applications for Aviation Weather. *Pure Appl. Geophys.* **2019**, *176*, 1959–1976. [[CrossRef](#)]
3. Zheng, Z.; Zhao, C.; Zhang, H.; Yang, S.; Zhang, D.; Yang, H.; Liu, J. Phase Noise Reduction by Using Dual-Frequency Laser in Coherent Detection. *Opt. Laser Technol.* **2016**, *80*, 169–175. [[CrossRef](#)]
4. Mocker, H.W.; Bjork, P.E. High Accuracy Laser Doppler Velocimeter Using Stable Long-Wavelength Semiconductor Lasers. *Appl. Opt.* **1989**, *28*, 4914. [[CrossRef](#)]
5. Churnside, J.H. Laser Doppler Velocimetry by Modulating a CO<sub>2</sub> Laser with Backscattered Light. *Appl. Opt.* **1984**, *23*, 61. [[CrossRef](#)] [[PubMed](#)]
6. Morvan, L.; Lai, N.D.; Dolfi, D.; Huignard, J.-P.; Brunel, M.; Bretenaker, F.; Le Floch, A. Building Blocks for a Two-Frequency Laser Lidar-Radar: A Preliminary Study. *Appl. Opt.* **2002**, *41*, 5702. [[CrossRef](#)] [[PubMed](#)]
7. Diaz, R.; Chan, S.-C.; Liu, J.-M. Lidar Detection Using a Dual-Frequency Source. *Opt. Lett.* **2006**, *31*, 3600. [[CrossRef](#)] [[PubMed](#)]
8. Lavrič, A.; Batagelj, B.; Vidmar, M. Calibration of an RF/Microwave Phase Noise Meter with a Photonic Delay Line. *Photonics* **2022**, *9*, 533. [[CrossRef](#)]
9. Diaz, R.; Chan, S.-C.; Liu, J.-M. *Dual-Frequency Multifunction Lidar*; Mecherle, S., Korotkova, O., Eds.; SPIE: San Jose, CA, USA, 2007; p. 645700.
10. Chen, G.; Lu, D.; Guo, L.; Zhao, W.; Wang, H.; Zhao, L. Dual-Frequency Laser Doppler Velocimeter Based on Integrated Dual-Mode Amplified Feedback Laser. In *Proceedings of the 2018 Asia Communications and Photonics Conference (ACP), Hangzhou, China, 26–29 October 2018*; IEEE: Piscataway, NJ, USA, 2018; pp. 1–3.
11. Onori, D.; Scotti, F.; Scaffardi, M.; Bogoni, A.; Laghezza, F. Coherent Interferometric Dual-Frequency Laser Radar for Precise Range/Doppler Measurement. *J. Light. Technol.* **2016**, *34*, 4828–4834. [[CrossRef](#)]
12. Wang, L.; Zhao, L.; Zhang, Y.; Wu, Y.; Xia, H. Tunable Dual-Frequency Coherent Doppler Lidar Using Bi-Directional Electro-Optic Modulation in a Sagnac Loop. *Opt. Commun.* **2023**, *526*, 128852. [[CrossRef](#)]
13. Cheng, C.-H.; Lee, C.-W.; Lin, T.-W.; Lin, F.-Y. Dual-Frequency Laser Doppler Velocimeter for Speckle Noise Reduction and Coherence Enhancement. *Opt. Express* **2012**, *20*, 20255–20265. [[CrossRef](#)] [[PubMed](#)]
14. Vercesi, V.; Onori, D.; Laghezza, F.; Scotti, F.; Bogoni, A.; Scaffardi, M. Frequency-Agile Dual-Frequency Lidar for Integrated Coherent Radar-Lidar Architectures. *Opt. Lett.* **2015**, *40*, 1358. [[CrossRef](#)] [[PubMed](#)]
15. Bai, Y.; Ren, D.; Zhao, W.; Qu, Y.; Qian, L.; Chen, Z. Heterodyne Doppler Velocity Measurement of Moving Targets by Mode-Locked Pulse Laser. *Opt. Express* **2012**, *20*, 764–768. [[CrossRef](#)] [[PubMed](#)]
16. Jang, Y.-S.; Kim, S.-W. Distance Measurements Using Mode-Locked Lasers: A Review. *Nanomanuf. Metrol.* **2018**, *1*, 131–147. [[CrossRef](#)]

**Disclaimer/Publisher's Note:** The statements, opinions and data contained in all publications are solely those of the individual author(s) and contributor(s) and not of MDPI and/or the editor(s). MDPI and/or the editor(s) disclaim responsibility for any injury to people or property resulting from any ideas, methods, instructions or products referred to in the content.